TRANSITION METAL–CHALCOGEN SYSTEMS IX: THE VANADIUM–TELLURIUM SYSTEM — PHASE DIAGRAM AND MAGNETIC PROPERTIES*†

PETER TERZIEFF and HERBERT IPSER

Institut für Anorganische Chemie der Universität Wien, A-1090 Wien (Austria)

ERNST WACHTEL

Max-Planck-Institut für Metallforschung, Institut für Werkstoffwissenschaften, D-7000 Stuttgart 1 (F.R.G.)

Summary

The V–Te phase diagram has been studied by differential thermal analysis, X-ray powder diffraction, and magnetic susceptibility measurements with emphasis on the phase boundaries within the $NiAs$–CdI_2-type phase field. The appearance of a high temperature modification of monoclinic V_3Te_4 has been observed, possibly with an undistorted CdI_2-like structure. The transition is reversible with a maximum transition temperature of 1180 K located at the stoichiometric composition V_3Te_4. The magnetic properties of the high temperature phase are characterized by a Curie–Weiss-like behaviour.

1. Introduction

The broad phase field of metal deficient $NiAs$–CdI_2-type $V_{1-x}Te$ is split into several regions distinguished by characteristic arrangements of the vacant metal sites. The first systematic investigation performed by Grønvold et al. [1] disclosed complex phase relationships as indicated by the appearance of four different phases. The hexagonal $NiAs$-type phase γ_1 was found to be stable at high temperatures in a narrow composition range around V_7Te_8 (53.3 at.% Te), whereas the monoclinically distorted version γ_2 had a broad range of homogeneity centred around stoichiometric V_3Te_4. Another hexagonal phase, γ_3, with an undistorted CdI_2 structure was assumed to exist at high temperatures in a narrow composition range slightly below 64 at.% Te. The structure of the tellurium-rich phase γ_4, stable in the composition range near VTe_2, was identified as an orthorhombic variant of the CdI_2-type structure. Almost at the same time Ukrainskii *et al.* [2] performed an X-ray

---

*Dedicated to Professor Dr. A. Neckel on the occasion of his 60th birthday.
†Transition metal–chalcogen systems VIII: the Cr–Te phase diagram was published as *J. Less-Common Met., 92* (1983) 263.

investigation of the system and arrived at quite different results. This prompted Røst *et al.* [3] to a reinvestigation confirming most of the earlier findings of Grønvold *et al.* [1]. Additionally, they reported the formation of a new monoclinic phase with the stoichiometry V_2Te_3. Furthermore, it was argued that the orthorhombic structure of γ_4 proposed by Grønvold *et al.* [1] could actually be monoclinically deformed with an angle β very close to 90°. Brunie and Chevreton [4] detected another monoclinic superstructure with the stoichiometric composition V_5Te_8, which was considered to be identical with the phase V_2Te_3 claimed by Røst *et al.* [3]. Recently, Bronsema *et al.* [5] arrived at the conclusion that the true structure of VTe_2 is monoclinic, isostructural with $NbTe_2$. The high temperature form of VTe_2 was determined to be the simple undistorted CdI_2-type structure.

In the past much attention has been paid to the magnetic properties of the $NiAs-CdI_2$-type vanadium tellurides but with emphasis primarily on the low temperature range and the stoichiometric compositions. Røst *et al.* [3] observed a pronounced cusp-like anomaly in the magnetic susceptibility in samples containing more than 61 at.% Te. In view of the resemblance to the χ *versus* T curves of typical antiferromagnets, the anomalies were attributed to the onset of antiferromagnetic interactions. Based on X-ray diffraction, magnetic susceptibility, electrical resistivity and thermal analysis, Ohtani *et al.* [6] identified these effects as reversible first-order transformation induced presumably by charge density waves. Anzai and coworkers [7, 8] focused their interest on the low temperature behaviour and classified both V_3Te_4 and V_5Te_8 as weakly correlated itinerant antiferromagnets.

Our own preliminary differential thermal analysis (DTA) measurements yielded thermal effects in the high temperature range of V_3Te_4 indicating the occurrence of a phase transformation. In view of the more or less rudimentary character of the phase diagram we considered it worthwhile to investigate this hitherto unknown phase transition with the help of DTA and magnetic measurements. While our investigation was in progress, Ohtani *et al.* [9] proposed a phase diagram which confirmed some of our preliminary findings.

2. Experimental details

Vanadium foil with a purity better than 99.8% (Goodfellow Metals, England) and tellurium lumps with 99.999% purity (Alfa-Ventron, MA, U.S.A.) were used as starting materials. Appropriate amounts of the pure elements were mixed, repeatedly evacuated, flushed with titanium-gettered argon, and finally sealed in quartz ampoules under a vacuum of about 0.01 Pa. Because of the reaction with the quartz, alloys containing less than 55 at.% Te were placed in alumina containers to prevent direct contact between the samples and the quartz ampoules. The mixtures were heated in steps to about 1350 K; after a reaction period of a few days the samples were cooled, ground and subjected once more to the above sealing pro-

cedure. In general, alloys used for the magnetic measurements were homogenized at 1100 K for about three weeks and subsequently quenched in ice–water, whereas the DTA samples were annealed at about 700 K for a comparable time. The completeness of the reaction was checked by X-ray diffraction in Debye–Scherrer cameras (diameter, 57.3 mm) using Co Kα radiation and iron filters.

The thermal analyses were performed on commercial equipment (DTA 404S/3; Netzsch, F.R.G.) using samples of about 0.5 g sealed under vacuum in specially designed quartz containers. In general, our data refer to a heating or cooling rate of 2 K min^{-1}, but at temperatures above 1300 K a rate of 10 K min^{-1} was preferred so as to minimize the exposure of the sample and the quartz ampoule to these high temperatures. Either pure chromium or an empty alumina crucible was used as reference material. The temperature was measured with Pt–Pt10%Rh thermocouples, calibrated at the melting points of high purity zinc, antimony and gold.

Suitable quartz containers had also to be used for the magnetic measurements which were conducted on an automatically compensating Faraday-type balance designed by Beisswenger and Wachtel [10]. The contribution of the sealed quartz ampoules to the magnetic susceptibility, inaccessible to direct measurements, was determined by measuring a series of empty ampoules; owing to the strict proportionality between the mass of the ampoule and the compensating force the contribution of the quartz ampoules could be calculated with sufficient accuracy. The magnetic susceptibilities were recorded both on heating and cooling between room temperature and 1350 K at a rate of 5 K min^{-1}. The structure of those samples which had been subjected to the magnetic measurements was identified by the Guinier X-ray diffraction technique (Enraf–Nonius, FR552) using Cu Kα radiation and silicon as an internal standard. As a consequence, if not stated otherwise, the heat treatment of the alloys used for the X-ray investigation refers basically to slow cooling from 1350 K at a rate of 5 K min^{-1}, as obtained during the magnetic measurements.

3. Results and discussion

On account of the high vapour pressure of tellurium all samples had to be sealed in quartz ampoules; consequently, our investigations were confined to an upper temperature limit of about 1500 K. The invariant arrests, the solidus and liquidus temperatures, and the other thermal effects are listed separately in Table 1; with the exception of the liquidus temperatures all values were obtained from the heating curves. The assignment of the observed effects to the phase diagram is shown in Fig. 1 (except in the central range where they are left out for the sake of clarity). The tellurium-rich eutectic was found to be 6 K below the melting point of pure tellurium (723 K) located at a composition very close to 100 at.% Te. The liquidus temperatures increase rapidly with decreasing tellurium content reaching

TABLE 1

Results of differential thermal analysis

Composition (at.% Te)	Invariant thermal arrests (K)	Other effects (K)	Solidus (K)	Liquidus	
				Heating (K)	Cooling (K)
44.1	No thermal effect detectable up to 1523 K				
46.0	No thermal effect detectable up to 1528 K				
48.0	1022				
50.0	1023				
51.9	1018				
54.5	1027				
55.5	1025				
55.9		1118 - 1122[a]			
56.5		1161 - 1170[a]			
57.0		1169 - 1174[a]			
57.3		1176 - 1181[a]			
57.6		1176 - 1180[a]			
58.1		1173 - 1176[a]			
58.6		1150 - 1154[a]			
58.8		1151 - 1156[a]			
59.0		1127 - 1133[a]			
59.2		1134 - 1138[a]			
59.5		1120 - 1123[a]			
59.9		1112 - 1115[a]	1494		
60.3		1097 - 1101[a]	1445		
60.5		1081 - 1083[a]	1416		
60.7		1077 - 1079[a]	1414		
61.5		825, 1044	1370		
62.1		992	1330		
63.0			1276		
63.5			1250		
64.0			1221		
64.5		411 - 423[a]	1187		
65.0		414 - 432[a]	1171		
65.5		438 - 446[a]	1111		
66.0		435 - 440[a]	~ 973		
67.5	479, 716				
70.0	480, 717			1553	1536
72.5	481, 715			1492	1451
75.0	480, 718			1448	1409
77.5	478, 716			1343	1309
79.9	479, 717			1248	1249
82.6	481, 716			1216	1184
85.1	480, 717			1176	1159
87.5	477, 716			1063	1059
90.1	481, 718			1079	999
92.3	476, 716			943	908
94.9	483, 718			878	813
97.3	473, 715			—	799

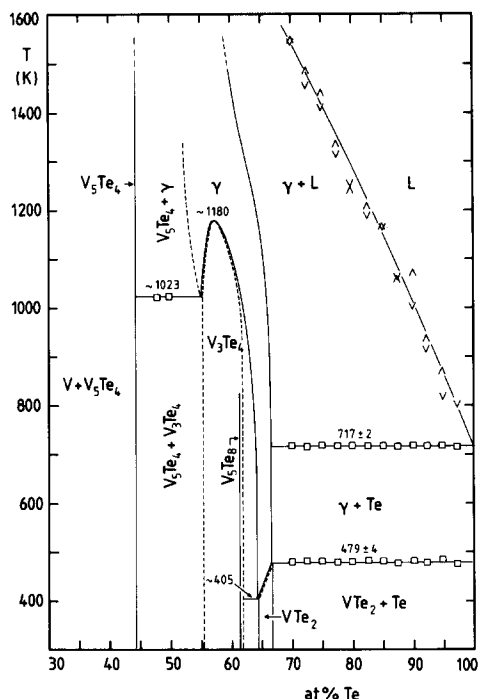[a]The first number indicates the beginning and the second the maximum of the peak in the ΔT curve on heating.

Fig. 1. The V—Te phase diagram in the range from 30 to 100 at.% Te (□ invariant arrests; ∧, ∨ liquidus temperatures obtained on heating and cooling, respectively).
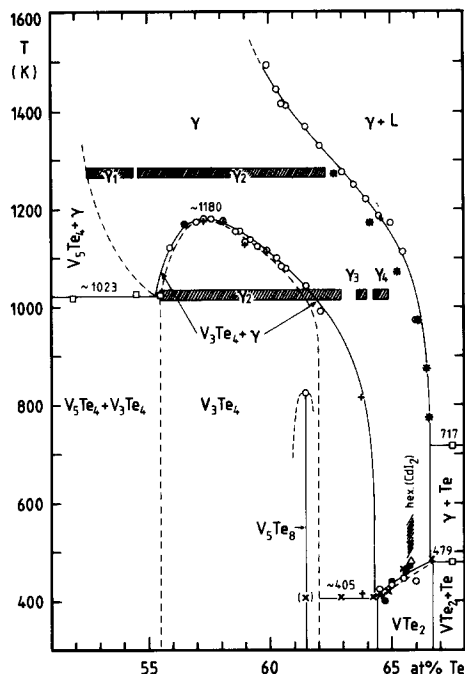
Fig. 2. Partial V—Te phase diagram in the range of the NiAs—CdI$_2$-type phase (○, □, thermal effects; +, magnetic effects; *, thermodynamically deduced phase boundary [11]; ×, △, ●, literature data from refs. 3, 5 and 6 respectively).

about 1550 K at 70 at.% Te. The values obtained on heating and cooling are distinguished by different symbols (∧, ∨). The details in the region of the phases with NiAs-derivative structures are shown more explicitly in Fig. 2 including all experimental data points. The position of the solidus curve on the tellurium-rich side is in acceptable agreement with the phase boundary deduced from the thermodynamic measurements (*) [11]. An extrapolation of this curve and of the corresponding liquidus curve indicates that a possible congruent melting point has to be between at least 1800 and 2000 K if not higher. The invariant arrest observed at 479 K is attributed to the peritectoid decomposition of monoclinic VTe$_2$ into tellurium and γ-V$_{1-x}$Te, a high temperature modification probably with a hexagonal CdI$_2$-type structure [5]. Several thermal effects with variable intensities indicated the transition from the monoclinic to this hexagonal structure which was suggested to be of first order [6]. As already observed by others [3, 6], the magnetic susceptibility was found to be a very sensitive indicator of this type of phase transformation, thus the phase boundary between VTe$_2$ and γ-V$_{1-x}$Te seems to be well established. As shown in Fig. 3, the alloy with 64.6 at.% Te gives an example of the marked discontinuities
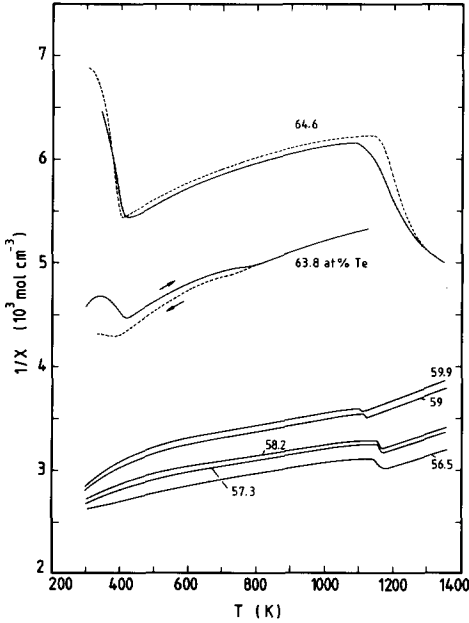
Fig. 3. The inverse magnetic susceptibility of the NiAs–CdI$_2$-type vanadium tellurides as function of temperature.
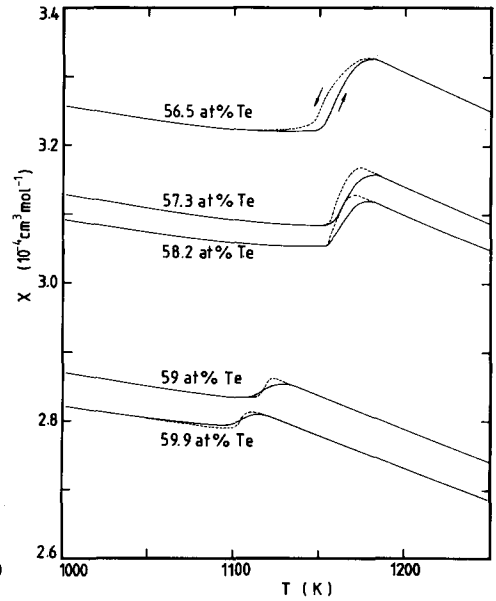
Fig. 4. The variation in the magnetic susceptibility of the vanadium tellurides in the vicinity of the phase transformation of V$_3$Te$_4$.

between 400 and 480 K which have been assigned to a first-order discontinuous charge density wave transition [6], similar to that observed in VSe$_2$ [12, 13]. In fact, following the empirical rule worked out by Thompson [4] the charge density wave transition temperature should be linearly correlated with the axial ratio of the hexagonal cell. Taking the axial ratios of 1.81 at 65.8 at.% Te as determined by Bronsema et al. [5] and 1.75 obtained in this paper for 64.6 at.% Te we would indeed expect phase transitions at 450 K and 330 K, respectively. This is in acceptable agreement with the transition temperatures deduced from the magnetic measurements. In addition to our own values (○, +) we also included in Fig. 2 the results given by Røst et al. [3] (X), Ohtani et al. [6] (●) and Bronsema et al. [5] (△) which are obviously in good agreement.

The most striking features are the thermal effects observed at high temperatures in the range between 56 and 63 at.% Te pointing definitely to the existence of a high temperature modification of monoclinic V$_3$Te$_4$. The transition temperatures pass through a characteristic maximum of 1180 K located near the stoichiometric composition V$_3$Te$_4$ (57.1 at.% Te). The occurrence of a phase transformation is also manifested by the very marked discontinuity in the magnetic susceptibility as shown in Fig. 4. The magnetically deduced transition temperatures are in excellent agreement with those based on thermal effects. We assumed this phase transition to be of first order with

a very narrow two-phase range which widens at lower temperatures. Concerning the structure of high temperature V_3Te_4 we assume a CdI_2-type structure, very similar to Cr_3Se_4 which definitely undergoes such a transformation from an ordered monoclinic to a partially disordered hexagonal CdI_2-like structure [15]. The phase relationships between NiAs-type γ_1 and the CdI_2-type high temperature versions of monoclinic V_3Te_4 and VTe_2 are unclear, but it cannot be excluded that they represent one single phase. In order to simplify the further discussion we designate the whole high temperature phase range as NiAs–CdI_2 type γ-$V_{1-x}Te$. Despite the obvious similarity to the situation in Cr_3Se_4 and the appearance of two other NiAs–CdI_2-like phases, i.e. γ_1 and γ_3, the ultimate answer can only be given by high temperature X-ray diffraction experiments.

The invariant arrests at 1023 K are most likely associated with the eutectoid decomposition of γ into V_3Te_4 and monoclinic V_5Te_4. This latter phase itself is shown in Fig. 1 as a line compound at the stoichiometric composition (44.4 at.% Te), since previous X-ray studies [1, 3] indicated a very narrow homogeneity range. No thermal effects could be observed in samples with 44.1 and 46 at.% Te up to about 1525 K; therefore it must be concluded that the melting or decomposition point of V_5Te_4 lies above this temperature.

The X-ray diffraction pattern of alloys between 56 and 62 at.% Te could be indexed unambiguously with a monoclinic supercell related to the primitive hexagonal cell (a', c') by $a \approx a'\sqrt{3}$, $b \approx a'$, $c \approx 2c'$, and $\beta \neq 90°$. The alloys with 62.1 and 63 at.% Te showed the diffuse diffraction pattern of V_3Te_4 with changed intensities caused by the superposition of some lines belonging to a second phase. The sample with 63.8 at.% Te clearly contained the pattern of a hexagonal CdI_2-type phase which turned out to be the main component at 64.6 at.% Te. Debye–Scherrer X-ray photographs of quenched alloys with 63.5, 64 and 64.7 at.% Te yielded similar results. Therefore we are inclined to assume that the two-phase range where γ and V_3Te_4 coexist extends at 600 K from about 62 to 64 at.% Te, in contrast to its extremely narrow width at higher temperatures. Accordingly, we assigned the discontinuity at 815 K observed in the χ^{-1} versus T curve of the alloy with 63.8 at.% Te to the phase boundary between γ and $\gamma + V_3Te_4$ (see Fig. 3). From the pronounced minima apparent in the χ^{-1} versus T curves at 63.8 and 64.6 at.% Te, which seem to accompany the formation of low temperature VTe_2, we must infer that this phase has actually formed, although the diffraction pattern still contained the hexagonal component, most probably due to an incomplete reaction. Our observations support the findings of Røst et al. [3] who suggested a two-phase range indicated by the constancy of the transition temperature. It is peculiar that in the range from 62 to 64 at.% Te the phase transitions are not accompanied by thermal effects large enough to be detected by our DTA measurements, a fact already observed by Ohtani et al. [6]. Concerning the true low temperature equilibrium, it seems to be plausible that V_5Te_8 might be involved instead of V_3Te_4, as proposed by Ohtani et al. [9]. However, possibly owing to our
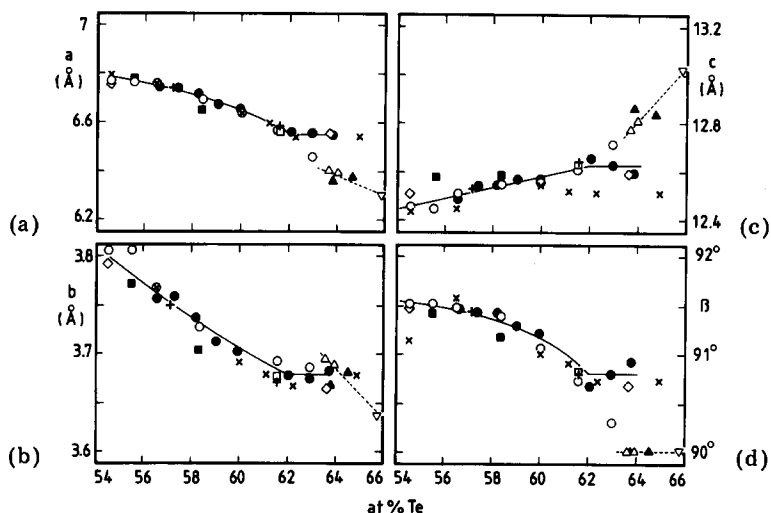
Fig. 5. Lattice parameters of NiAs–CdI$_2$-type vanadium tellurides as a function of composition ($\bullet$, $\blacktriangle$, this work; $\circ$, $\times$, $\diamond$, $\triangle$ are taken from ref. 1; $\blacksquare$ from ref. 3; $\square$ from ref. 4; $\triangledown$ from ref. 5; + from refs. 7 and 8; $\blacktriangle$, $\triangle$, $\triangledown$ refer to the hexagonal cell).

high cooling rates (5 K min^{-1} for the magnetic measurements, 2 K min^{-1} for the thermal analyses) we could not observe the appearance of V$_5$Te$_8$, except at 61.5 at.% Te where a thermal effect at 825 K indicated the formation of a new phase (see Fig. 2). Indeed, after annealing the alloy with 61.5 at.% Te at 720 K for about three days we obtained the diffraction pattern of V$_5$Te$_8$ reported by Brunie and Chevreton [4].

The variation of the lattice parameters with the composition is illustrated in Fig. 5, where our own data ($\bullet$, slowly cooled) are compared with those of Grønvold et al. [1] ($\times$, quenched from 1270 K; $\circ$, quenched from 1020; $\diamond$, slowly cooled), Røst et al. [3] ($\blacksquare$, slowly cooled), Brunie and Chevreton [4] ($\square$, quenched from 1070 K) and Anzai and coworkers [7, 8] (+, quenched from 1020 K). We also included the hexagonal parameters by using an orthorhombic description of the hexagonal cell. The scattering of the data, most evident in the two-phase range, is to some extent due to the different thermal treatments of the samples. The breaks near 62 at.% Te indicate apparently the tellurium-rich phase limit of V$_3$Te$_4$. The hexagonal parameters obtained for slowly cooled ($\blacktriangle$, this work) and quenched alloys ($\triangle$, quenched from 1020 K [1]) correlate with those measured directly above 482 K by Bronsema et al. [5]. As already pointed out by others [4, 8], the structure of V$_5$Te$_8$, obtainable only by extremely slow cooling, differs from V$_3$Te$_4$ by a reduced a and an increased c. Our own lattice parameters ($a = 12.880$ Å, $b = 7.584$ Å, $c = 12.591$ Å, $\beta = 90.9°$) are nearly identical with the values given by Brunie and Chevreton [4] ($a = 12.874$ Å, $b = 7.580$ Å, $c = 12.630$ Å, $\beta = 90.8°$) and only slightly different from those reported by Anzai and Ohta [8] ($a = 12.85$ Å, $b = 7.57$ Å, $c = 12.61$ Å, $\beta = 90.9°$).

The position of the different phases reported by Grϕnvold *et al.* [1] and the regions where they have been observed are shown by the hatched stripes in Fig. 2. Inasmuch as the hexagonal NiAs-type phase γ_1 is concerned our results confirm the existence of such a phase. An alloy with 53.3 at.% Te (V_7Te_8) quenched from 1070 K was clearly a two-phase mixture containing a hexagonal NiAs-like phase as the major component. Our lattice parameters ($a = 3.959$ Å, $c = 6.147$ Å) are not far from those given by Grϕnvold *et al.* [1] ($a = 3.942$ Å, $c = 6.126$ Å) which refer to a different quenching temperature (1270 K) and a different composition. We contend that in the high temperature regime the transition from γ to V_3Te_4 cannot be suppressed by normal quenching, which explains why Grϕnvold *et al.* [1] obtained their γ_2 (V_3Te_4) by quenching from 1270 K. We confirm the existence of their high temperature phase γ_3 with a CdI_2-like structure, but we found neither evidence of the orthorhombic phase γ_4, nor the monoclinic version of VTe_2 reported by Rϕst *et al.* [3]. Bronsema *et al.* [5] have proposed a different monoclinic structure of VTe_2 which seems to be related to both the orthorhombic structure observed by Grϕnvold *et al.* [1] and the monoclinic version reported by Rϕst *et al.* [3]. In fact, a sample with 66 at.% Te annealed at 420 K for four weeks could be indexed with the monoclinic cell given by Bronsema *et al.* [5]. Our lattice parameters ($a = 19.057$ Å, $b = 3.609$ Å, $c = 9.074$ Å, and $\beta = 134.68°$) are very close to the values cited by Ohtani *et al.* [9] ($a = 19.041$ Å, $b = 3.613$ Å, $c = 9.079$ Å, $\beta = 134.63°$) but differ from those reported by Bronsema *et al.* [5] ($a = 18.894$ Å, $b = 3.595$ Å, $c = 9.069$ Å, $\beta = 134.62°$) most likely because of a difference in composition.

In contrast to our version, Ohtani *et al.* [9] proposed a eutectoid decomposition at about 800 K of the high temperature CdI_2-type γ-phase into V_3Te_4 and β-VTe_2, a phase with a hitherto unknown structure stable at intermediate temperatures. According to their results the transition from β to γ VTe_2 was found to be reflected by the magnetic susceptibility which seemed to increase on heating above 1000 K indicating the formation of the high temperature CdI_2-type phase. At nearly the same composition (64.6 at.% Te) our own measurements yielded a smooth curve, devoid of any anomalies, from 400 K up to the solidus temperature which is manifested by the abrupt decrease in the inverse magnetic susceptibility at 1180 K (*cf.* Fig. 2). Although our phase diagram and that of Ohtani *et al.* [9] differ in some respects, they also share some common features. Above all, they also observed the appearance of a high temperature form of V_3Te_4 which was assumed to be of the CdI_2 type. Their transition temperatures passed through a maximum at 55.6 at.% Te and 1145 K, whereas we observed the maximum located close to V_3Te_4 (57.1 at.% Te) and 1180 K. Moreover, although assuming two additional two-phase fields on account of their β-VTe_2, they also suggest a two-phase range between 61.5 and 63.6 at.% Te in reasonable agreement with our values.

The thermodynamic activities of tellurium over solid V–Te alloys have been recently determined between 54 and 66.7 at.% Te [11]. They were

related to a preliminary phase diagram based mainly on the results reported by Grønvold et al. [1]. It is evident that the isopiestic equilibrium curves (sample temperature *versus* sample composition) shown in Fig. 1 of ref. [11] and consequently the resulting activity curve have to be somewhat reinterpreted in view of the phase boundaries proposed in this paper. Both show a horizontal inflection point between about 62 and 65 at.% Te becoming more pronounced with decreasing temperature which was attributed to the appearance of a miscibility gap below 825 K. However, the shape of these curves can equally well be interpreted by a horizontal segment reflecting the two-phase field between V_3Te_4 and γ as determined in the present investigation. Furthermore, it should be mentioned that the vertical inflection point of the activity curve in the vicinity of the composition V_3Te_4 seems to conflict with the assumption of a continuous hexagonal phase field of the NiAs–CdI_2-type structure at high temperatures. For this particular case a similar shape as obtained in the Ni–Te [16] and Co–Te [17] systems would have been expected, where this continuous phase has been well established.

In the past two decades the understanding of the magnetic properties has changed fundamentally. From the concave curvature of the χ^{-1} *versus* T curves Røst et al. [3] assumed a ferrimagnetic character of V_3Te_4, whereas the susceptibility maximum of VTe_2 seemed to indicate antiferromagnetic interactions. Meanwhile, owing to the work of Anzai and coworkers [7, 8], both stoichiometric V_3Te_4 and V_5Te_8 are classified as weak itinerant antiferromagnets. The susceptibility cusp of VTe_2, which is indeed strikingly similar to the susceptibility curve of a classical antiferromagnet near the Néel temperature, is assigned to a first-order charge density wave transition. Ohtani and coworkers [6, 15] and Anzai and Ohta [8] were successful in describing the magnetic susceptibility in terms of a Curie–Weiss-like expression: $\chi = \chi_0 + C/(T - \theta)$, where χ_0 is a temperature-independent term; C is the Curie constant and θ is the paramagnetic Curie temperature. For the low temperature regime they obtained magnetic moments (not more than 1 μ_B) much smaller than expected from a localized picture (2.83 μ_B for V^{3+} or 3.87 μ_B for V^{2+}). Our own attempts to fit the high temperature susceptibility by such a Curie–Weiss-like expression resulted in the magnetic parameters given in Table 2. We obtained small magnetic moments ranging from 0.59 μ_B at 64.6 at.% Te to 1.62 μ_B at 56.5 at.% Te which indicates a high degree of delocalization. It has been suggested that only the vanadium atoms of the partially filled layers contribute to the magnetic moment, while those of the fully occupied layers are responsible for the itinerant character [9]. This would indeed explain the small magnetic moments. The constant term χ_0 seems to be high compared with the total magnetic susceptibility reflecting a high density of states at the Fermi level. Excepting the alloys with 56.5 and 64.6 at.% Te the strong curvature below 400 K could not be reproduced accurately by assuming a Curie–Weiss-like behaviour, therefore our paramagnetic Curie temperatures have only a very limited physical significance. In fact, by comparing our data with those deduced from the low temperature behaviour [8, 9] we observe a discrepancy of about one

TABLE 2

Magnetic data of NiAs–CdI$_2$-type vanadium tellurides

Composition (at.% Te)	χ_0 (10^{-4} cm^3 mol^{-1})	C (cm^3 mol^{-1} K)	θ (K)	μ (μ_B (V atom)$^{-1}$)
56.5	2.43	0.143	−722	1.62
	—	(0.943)	(−1653)	(4.17)
57.3	2.53	0.087	−446	1.28
	—	(0.885)	(−1614)	(4.07)
58.2	2.61	0.065	−342	1.12
	—	(0.894)	(−1686)	(4.14)
59.0	2.45	0.052	−212	1.01
	—	(0.795)	(−1650)	(3.94)
59.9	2.46	0.042	−137	0.92
	—	(0.789)	(−1691)	(3.97)
63.8	1.56	0.038	−30	0.91
64.6	1.47	0.015	15	0.59

order of magnitude. Similar difficulties, deviations from a strict Curie–Weiss-like behaviour and a discrepancy with respect to the magnetic moments, were reported for the structurally related V_{1-x}Se, where the interpretation was given in terms of spin fluctuations [18]. This concept might also be applicable to V_{1-x}Te; therefore we abstain from overestimating the significance of the magnetically deduced parameters.

The high temperature modification of V_3Te$_4$ is distinguished by a strict linear relationship between χ^{-1} and T, in contrast to the low temperature version, where a constant value had to be subtracted in order to obtain an acceptable linear relationship. It cannot be excluded that the paramagnetic contribution of the itinerant electrons may be cancelled by the diamagnetic contribution of the core atoms. The magnetic parameters derived directly from the linearity between χ^{-1} and T are given in parentheses in Table 2. Surprisingly, the magnetic moments range from 3.97 to 4.17 μ_B per V-atom hinting at a localization of the d-electrons. The negative sign of the paramagnetic Curie-temperatures are indicative of antiferromagnetic interactions at low temperatures. Concerning the reliability of the magnetic data deduced for high temperature V_3Te$_4$ we have to admit that our conclusions are based on the very limited temperature range between 1150 and 1350 K. It would be of particular interest to extend the magnetic measurements to the temperature range above 1350 K. As far as our tentative phase diagram is concerned we emphasize that we tried to find the simplest version compatible with the observed effects. For a more complete phase diagram careful high temperature X-ray investigations focused on the structural details of the phase transition in V_3Te$_4$ and the phase relationships in the range of VTe$_2$ would be necessary.

Acknowledgments

References

1 F. Grønvold, O. Hagberg and H. Haraldsen, *Acta Chem. Scand.*, *12* (1958) 971.
2 Yu. M. Ukrainskii, A. V. Novoselova and Yu. P. Simanov, *Nauchn. Dokl. Vyssh. Shk., Khim. Khim. Tekhnol.*, (1959) 62.
3 E. Røst, L. Gjertsen and H. Haraldsen, *Z. Anorg. Allg. Chem.*, *333* (1964) 301.
4 S. Brunie and M. Chevreton, *Bull. Soc. Fr. Mineral. Cristallogr.*, *91* (1968) 422.
5 K. D. Bronsema, G. W. Bus and G. A. Wiegers, *J. Solid State Chem.*, *53* (1984) 415.
6 T. Ohtani, K. Hayashi, M. Nakahira and H. Nozaki, *Solid State Commun.*, *40* (1981) 629.
7 S. Anzai, S. Ohta, A. Yoshino, J. Nishio and M. Hatori, *Phys. Status Solidi B*, *118* (1983) K99.
8 S. Anzai and S. Ohta, *J. Phys. Soc. Jpn.*, *49* (1980) 2079.
9 T. Ohtani, S. Onoue and M. Nakahira, *Mater. Res. Bull.*, *19* (1984) 1367.
10 H. Beisswenger and E. Wachtel, *Z. Metallkd.*, *46* (1955) 504.
11 H. Ipser, *J. Solid State Chem.*, *54* (1984) 114.
12 M. Bayard and M. J. Sienko, *J. Solid State Chem.*, *19* (1976) 325.
13 A. H. Thompson and B. G. Silbernagel, *Phys. Rev. B*, *19* (1979) 3420.
14 A. H. Thompson, *Phys. Rev. Lett.*, *34* (1975) 520.
15 T. Ohtani, R. Fujimoto, H. Yoshinaga and M. Nakahira, *J. Solid State Chem.*, *48* (1983) 161.
16 M. Ettenberg, K. L. Komarek and E. Miller, *J. Solid State Chem.*, *1* (1970) 583.
17 R. M. Geffken, K. L. Komarek and E. Miller, *J. Solid State Chem.*, *4* (1972) 153.
18 Y. Kitaoka and H. Yasuoka, *J. Phys. Soc. Jpn*, *48* (1980) 1460.